EFFECT OF SINTERING TEMPERATURE ON THE MICROSTRUCTURE AND PROPERTIES OF Y₂O₃-DOPED SIAION CERAMICS

Tran Van Cuong1*, Ninh Duc Ha1, Dang Quoc Khanh2

¹Institute of Chemistry and Material, Military Academy of Science and Technology

²HaNoi University of Science and Technology

ARTICLE INFO		ABSTRACT		
Received:	15/4/2025	High-quality SiAlON ceramics are essential for advanced engineering		
Revised:	31/5/2025	applications owing to their outstanding mechanical, thermal, and chemical properties. Furthermore, tailored SiAlON compositions have shown		
Published:	31/5/2025	significant potential in electronic substrates and sensor technologies. In		
KEYWORDS		this study, Y ₂ O ₃ -doped SiAlON ceramics were synthesized via a conventional solid-state reaction method. The influence of sintering temperature on the physical properties of the ceramics was systematically		
Y ₂ O ₃ doped		investigated using X-ray diffraction, scanning electron microscopy, and		
SiAlON ceramic		fracture toughness measurements ($K_{\rm IC}$). Results revealed that increasing		
Si ₃ N ₄ ceramic		the sintering temperature from 1450 °C to 1650 °C led to a notable		
Microstructure		improvement in material densification, with bulk density increasing from $2.21 \pm 0.1 \text{ g/cm}^3$ to $2.66 \pm 0.1 \text{ g/cm}^3$. Concurrently, open porosity		
Sintering temperature		decreased from $11.07 \pm 0.20\%$ to $7.95 \pm 0.20\%$, and water absorption reduced from $4.99 \pm 0.20\%$ to $2.99 \pm 0.20\%$. These findings confirm the effective synthesis of high-quality Y_2O_3 -doped SiAlON ceramics with enhanced physical properties, underscoring their suitability for high-performance applications.		

ẢNH HƯỞNG CỦA NHIỆT ĐỘ THIỀU KẾT ĐẾN CẦU TRÚC VI MÔ VÀ TÍNH CHẤT CỦA GỐM SIAION-PHA TẠP Y_2O_3

Trần Văn Cương1*, Ninh Đức Hà1, Đặng Quốc Khánh2

 ^{1}V iện Hóa học - Vật liệu, Viện Khoa học và công nghệ Quân sự 2 Đại học Bách Khoa Hà Nội

THÔNG TIN BÀI BÁO		TÓM TẮT					
Ngày nhận bài:	15/4/2025	thuật tiên tiến nhờ các tính chất cơ học, nhiệt và hóa học đặc biệt của					
Ngày hoàn thiện:	31/5/2025						
Ngày đăng:	31/5/2025						
		gốm SiAlON pha tạp Y ₂ O ₃ được chế tạo bằng phương pháp phản ứng					
TỪ KHÓA		pha rắn thông thường. Bài báo đã nghiên cứu ảnh hưởng của nhiệt độ					
DI A MAG		thiêu kết đến các tính chất vật lý của gốm SiAlON pha tạp Y ₂ O ₃ bằng					
Pha tạp Y ₂ O ₃		phương pháp XRD, SEM và phép đo hệ số K _{IC} . Nghiên cứu này chỉ ra					
Gốm SiAlON		rằng khi nhiệt độ thiêu kết tăng từ 1450 °C đến 1650 °C, mật độ vật liệu					
Gốm Si₃N₄		tăng từ $2,21 \pm 0,1$ g/cm³ đến $2,66 \pm 0,1$ g/cm³ và độ xốp giảm từ $11,07 \pm 0$					
		0.20% xuống $7.95 \pm 0.20 \%$. Ngoài ra, khả năng hấp thụ nước giảm từ					
Vi cấu trúc		$4,99 \pm 0,20$ % xuống $2,99 \pm 0,20$ % khi nhiệt độ thiêu kết tăng từ 1450					
Nhiệt độ thiêu kết		°C đến 1650 °C. Kết quả của nghiên cứu chứng minh sự tổng hợp thành công gốm SiAlON chất lượng cao cho các ứng dụng tiên tiến.					

DOI: https://doi.org/10.34238/tnu-jst.12578

^{*} Corresponding author. Email: trancuong.hhvl@gmail.com

1. Introduction

SiAlON ceramics, a solid solution derived from Si₃N₄, have gained considerable attention due to their exceptional mechanical strength, thermal stability, and chemical resistance [1], [2]. These properties make them highly suitable for demanding applications such as cutting tools, engine components, and protective coatings [3]. The synthesis route and processing parameters, particularly the calcination and sintering conditions, play a crucial role in determining the final properties of SiAlON ceramics [4]. Recent studies have explored a range of synthesis strategies and their influence on SiAlON performance. For example, α-SiAlON phosphors doped with Eu²⁺ have been synthesized at 2050 °C under 0.92 MPa N₂ for white LED applications [5], while β-SiAlON porous ceramics have been fabricated via self-propagating high-temperature synthesis, reaching reaction temperatures of up to 1740 °C [6]. Additionally, Ca-α-SiAlON fine powders were prepared through a reductionnitridation route at 1400–1500 °C using an NH₃–CH₄ atmosphere [7]. Advances in sintering techniques, such as spark plasma sintering, have enabled the fabrication of oxygen-rich SiAlONs stabilized with various metal cations at 1500 °C [8]. Densified SiAlON ceramics with densities ranging from 3.17 to 3.92 g/cm³ have also been achieved using nano-sized precursors and spark plasma sintering. Conventional pressureless sintering at 1800 °C for up to 8 hours under 0.1 MPa N₂ has been employed to fabricate β-SiAlON ceramics with tailored Y₂O₃ contents [9], though formation of β-SiAlON phases often requires reaction temperatures exceeding 2000 °C [10]. Given the strong correlation between sintering temperature and SiAlON properties, systematic investigations are necessary to optimize processing parameters and improve material performance [11]. One-step gas pressure sintering at 1900 °C has been used to synthesize Eu-doped Ca-α-SiAlON phosphors [7], [12] - [13] while Nd-doped SiAlON ceramics have been fabricated via hot-press sintering at 1700 °C [14]. Moreover, the addition of rare earth additives such as Sm has been reported to reduce the phase formation temperature of β-SiAlON ceramics, with SmF₃ promoting densification and phase evolution at temperatures ≥ 1700 °C, yielding a maximum density of 2.6604 g/cm³ [15]. Traditionally, the synthesis of SiAlON ceramics demands high sintering temperatures (> 1800 °C). resulting in significant energy consumption and elevated processing costs. Therefore, strategies such as incorporating additives (e.g., Y₂O₃) or employing advanced precursors are being explored to improve processing efficiency and enhance the resulting properties [16]. Additive-assisted sintering affects phase composition, particle morphology, and densification behavior, all of which directly influence the mechanical and thermal performance of the final ceramics.

In this context, the present study investigates the effect of sintering temperature on the physical properties of Y₂O₃-doped SiAlON ceramics. The ceramics were synthesized using a conventional solid-state reaction method, with the objective of optimizing processing conditions to enhance densification, reduce porosity, and improve overall material performance.

2. Experiment

High-purity raw materials were used for the synthesis of SiAlON ceramics. The starting powders included silicon nitride (Si₃N₄, 98% purity, sourced from Vietnam), aluminum oxide (Al₂O₃, 98% purity, Vietnam), silicon dioxide (SiO₂, 99.99% purity, 175–225 m²/g surface area, Sigma-Aldrich, Product No. 381276), and yttrium oxide (Y₂O₃, 99.99% purity, Wako Pure Chemical Industries, Japan). The preparation procedure for SiAlON ceramics is schematically illustrated in Figure 1a.

The ceramic composition consisted of 90 wt% Si₃N₄, 0.49 wt% Al₂O₃, 8.51 wt% Y₂O₃, and 1 wt% SiO₂, and the corresponding sample was designated as 1A8Y1S_O. In a typical synthesis, the oxide precursors were weighed, mixed, and milled using a planetary ball mill (Fritsch Pulverisette, Germany). The milling was carried out at 130 revolutions per minute (rpm) for 2 hours using Si₃N₄ grinding media balls (φ: 5 mm), with a ball-to-powder weight ratio of 15:2. A solution of 5% polyvinyl alcohol (PVA) in dehydrated ethanol was used as a dispersant and binder during the

milling process. Following milling, the slurry was dried using a rotary evaporator to obtain homogeneously mixed powder. The dried powders were then uniaxially pressed into cylindrical pellets of 20 mm diameter and 20 mm height under a pressure of 200 MPa using a hydraulic press. The green compacts were subsequently machined into specimens with dimensions of 20 mm diameter \times 10 mm height. The sintering shrinkage behavior of the samples was evaluated using a high-temperature dilatometer (Linseis STA PT 1600, Germany) at a heating rate of 10 °C/min under a flowing nitrogen atmosphere (100 mL/min).

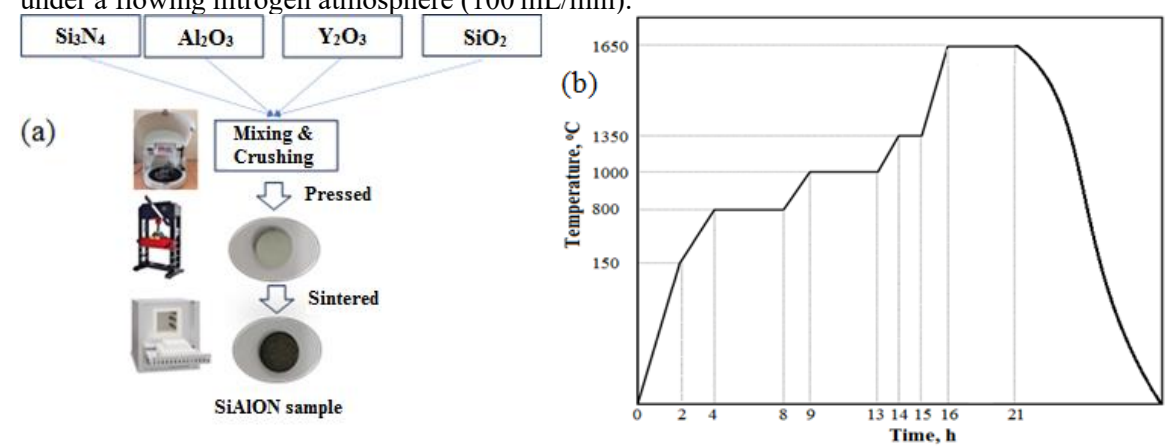


Figure 1. Diagram of processes and thermal treatment of SiAlON ceramic samples: a) diagram of processes; and b) thermal treatment

Sintering was performed at various temperatures (1450, 1500, 1550, 1600, and 1650 °C) for a total duration of 21 hours in a horizontal tube furnace (Gas Pressure Sintering, GPS, V-HEAT, Vietnam) under a nitrogen atmosphere at pressures ranging from 0.1 to 2.0 MPa. The furnace was heated at a rate of 3 °C/min, with a holding time of 5 hours at the target sintering temperature. During gas pressure sintering, the samples were placed in a graphite crucible (\$\phi\$100 mm internal diameter) coated with boron nitride (BN, 99%, China Abrasive Import & Export Corp., China) to prevent contamination and facilitate clean sintering. Details of the thermal processing steps are depicted in Figure 1b.

After cooling to room temperature, the phase composition and crystalline structure of the sintered samples were analyzed using X-ray powder diffraction (XRD; Bruker, Germany) with CuK α radiation (λ = 0.154 nm). Microstructural characterization was performed using scanning electron microscopy (SEM; Hitachi S-4800) to assess grain morphology, densification behavior, and phase distribution.

Bulk density and water absorption of the sintered ceramics were measured at 25 °C using the Archimedes method in accordance with the Vietnamese standard TCVN 6530-3:2016 [17]. Vickers hardness was determined following ASTM C1327 standards. Fracture toughness was evaluated based on surface crack lengths induced by Vickers indentation under a 3 kg load. Three indentations were made along the tensile axis at the center of the polished specimen surface, producing radial cracks with a total length of approximately 10 mm [18]. Elastic modulus testing was conducted using a mechanical testing setup (Kammrath & Weiss GmbH, Germany) mounted on an optical microscope stage (Model M11, Nikon Corporation, Japan). The fracture toughness was calculated using the Lihara equation, which correlates indentation-induced crack lengths with material toughness:

$$K_{1C} = 0.018 \left(\frac{E}{H\nu}\right)^{1/2} \left(\frac{P}{C^{3/2}}\right)$$
 (1)

Where: E is the elastic modulus, GPa; Hv is hardness, GPa; P is the compression pressure in N; c is 1/2 crack length (in mm).

3. Results and Discussion

The crystal structures and phase composition of the synthesized samples were investigated using X-ray diffraction (XRD). The XRD pattern of the 1A8Y1S_O sample sintered at 1650 °C is presented in Figure 2. The diffraction peaks clearly indicate the presence of two primary phases: α -SiAlON and β -SiAlON. In addition, minor impurity phases such as α -Si₃N₄, β -Si₃N₄, Y₂O₃·SiO₂, and 2Y₂O₃·Al₂O₃ were also detected. These results are in good agreement with previous reports on the synthesis of advanced SiAlON ceramics [19]- [20]. Notably, α -SiAlON, β -SiAlON, and α -Si₃N₄ phases have also been reported in SiAlON samples sintered at 1800 °C [21]. It has been documented that granular β -SiAlON begins to form at approximately 1550 °C and reaches near-complete formation at 1600 °C [22]. In this study, the formation of secondary phases is likely attributed to the high chemical reactivity of Y₂O₃, which interacts with SiO₂ and Al₂O₃ to produce Y₂O₃·SiO₂ and 2Y₂O₃·Al₂O₃ phases.

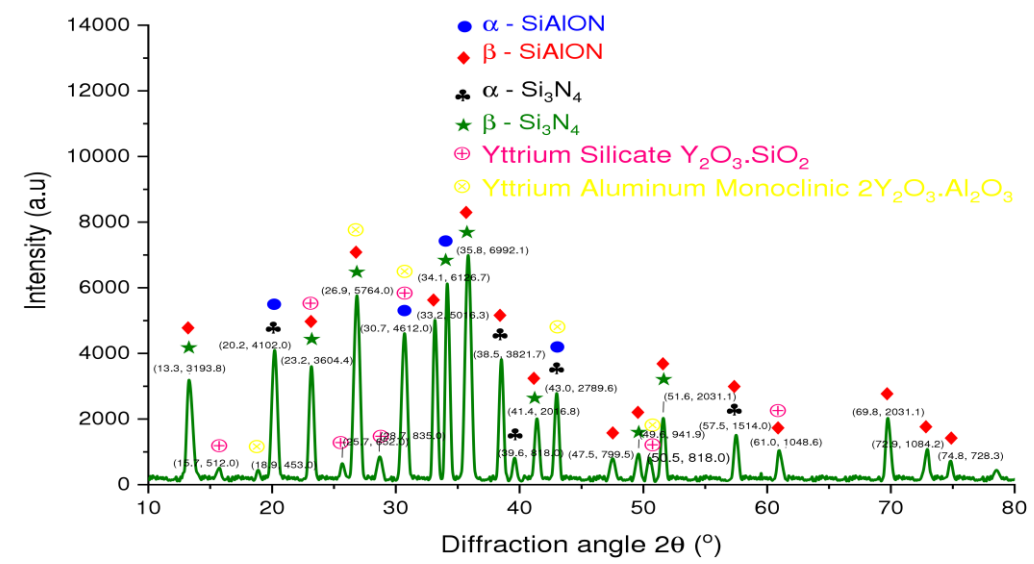


Figure 2. XRD patterns of the 1A8Y1S_O sample sintered at 1650 °C

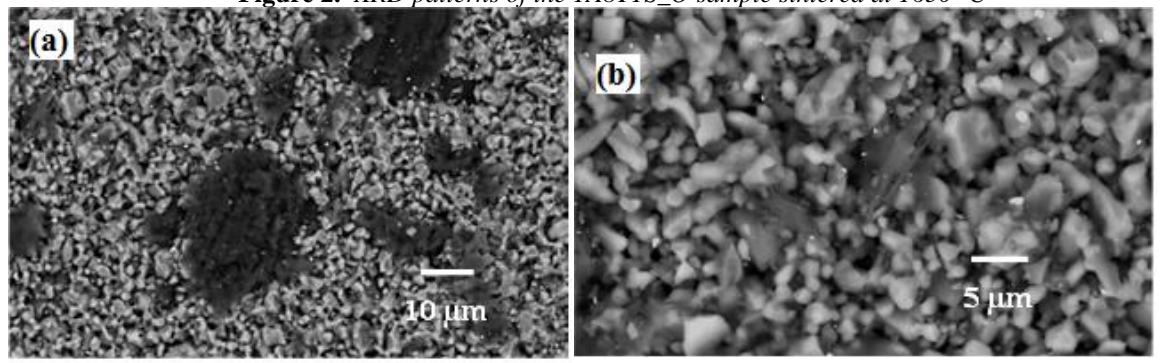


Figure 3. SEM images of the 1A8Y1S_O sample sintered at 1650 °C

The microstructural characteristics of the 1A8Y1S_O sample sintered at 1650 °C were examined using scanning electron microscopy (SEM), as shown in Figure 3. The low-magnification SEM image (Figure 3a) reveals a homogeneous microstructure consisting of fine grains predominantly in the sub-micron to several micron size range. The grains exhibit a well-defined morphology with distinct and sharp grain boundaries, suggesting effective phase development and crystallization during sintering. Consistent with the XRD results, some darker regions observed in the microstructure may correspond to residual secondary phases or localized impurity accumulation. Additionally, the presence of a few pores and voids is evident, which could

potentially affect the mechanical performance of the material, particularly its strength and fracture toughness. At higher magnification (Figure 3b), the SEM image provides a more detailed view of the grain morphology and distribution. While many grains exhibit well-defined boundaries, some regions display irregular grain shapes and less uniform densification. The visibility of small voids and darker inclusions becomes more pronounced at this scale, indicating areas of residual porosity or secondary phase formation. These microstructural features are likely to influence the overall mechanical strength, fracture resistance, and thermal stability of the SiAlON ceramic [23].

Processing temperature plays a critical role in influencing phase formation and the physical properties of SiAlON ceramics. As the sintering temperature increases, crystallization and phase transformation processes are enhanced, promoting densification and reducing porosity, which in turn improve the mechanical strength and durability of the ceramic material. In this study, the physical properties - specifically bulk density, porosity, and water absorption - of the synthesized SiAlON ceramics were systematically investigated as a function of sintering temperature. Figure 4 illustrates the temperature dependence of bulk density and porosity for samples sintered between 1450 °C and 1650 °C. A clear trend is observed: bulk density increases significantly from 2.21 \pm 0.10 g/cm³ to 2.66 \pm 0.10 g/cm³ as the sintering temperature rises. This densification behavior is primarily attributed to enhanced atomic diffusion at elevated temperatures, which facilitates stronger interparticle bonding and reduces pore volume. Additionally, grain rearrangement and volumetric shrinkage during sintering contribute to further minimization of porosity. The elevated temperatures also promote the removal of residual gases and transient liquid phases, thereby improving the overall compactness and structural integrity of the ceramics.

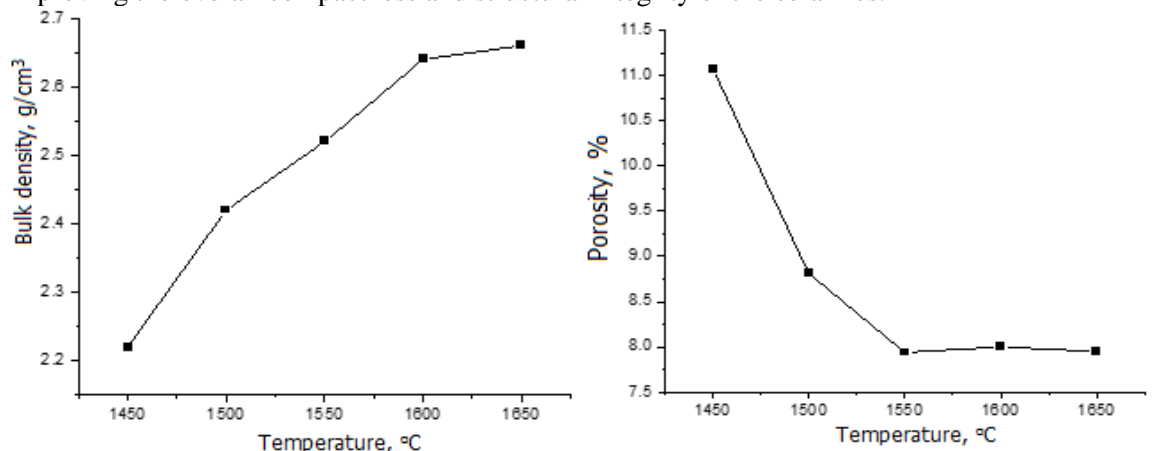


Figure 4. Effect of sintering temperatures on the bulk density of the SiAlON ceramics

Figure 5. Effect of sintering temperatures on the porosity of the SiAlON ceramics

In contrast to the trend observed in bulk density, the porosity of the SiAlON ceramics decreases markedly with increasing sintering temperature, as shown in Figure 5. Specifically, porosity decreases from $11.07 \pm 0.20\%$ to $7.95 \pm 0.20\%$ as the sintering temperature increases from $1450\,^{\circ}\text{C}$ to $1650\,^{\circ}\text{C}$. This reduction in porosity is primarily attributed to enhanced densification processes at elevated temperatures. Higher sintering temperatures intensify atomic diffusion, facilitating stronger interparticle bonding and the closure of voids. Moreover, grain growth and rearrangement during sintering contribute to a more compact microstructure, further reducing the amount of open pore space. Elevated temperatures also promote the elimination of residual gases and transient liquid phases, which otherwise contribute to porosity. The combined effect of these thermally activated processes leads to a significant improvement in the ceramic's structural integrity and overall material performance.

The Liquid Phase Sintering (LPS) method facilitates particle bonding through the formation of a transient liquid phase during the sintering process. This liquid phase enhances atomic diffusion,

promotes recrystallization via a dissolution—precipitation mechanism, and effectively fills interparticle voids. The main stages of LPS include: (i) heating to the sintering temperature, during which a portion of the fluxing agents (e.g., Y₂O₃ and SiO₂) melts to form a liquid phase; (ii) dissolution and recrystallization of SiAlON particles from the liquid; and (iii) cooling, leading to the stabilization of the microstructure.

The bulk density and porosity of SiAlON ceramics have a direct influence on the material's water absorption. The water absorption values for samples sintered at $1450\,^{\circ}\text{C}$, $1500\,^{\circ}\text{C}$, $1550\,^{\circ}\text{C}$, $1600\,^{\circ}\text{C}$, and $1650\,^{\circ}\text{C}$ are $4.99\pm0.20\%$, $3.64\pm0.20\%$, $3.16\pm0.20\%$, $3.03\pm0.20\%$, and $2.99\pm0.20\%$, respectively. A clear decreasing trend is observed with increasing sintering temperature. This reduction in water absorption is attributed to enhanced densification and reduced open porosity at higher temperatures, as corroborated by the corresponding increase in bulk density. The decrease in interconnected pores limits water ingress, thereby improving the material's structural performance. Additionally, the Vickers hardness and fracture toughness (K_{1C}) of the sintered SiAlON ceramics are summarized in Table 1. These mechanical properties further reflect the influence of sintering temperature on microstructural evolution and densification behavior.

Table 1. Effect of sintering temperatures on the hardness and fracture toughness of the SiAlON ceramics

Properties -	Temperature, °C						
	1450	1500	1550	1600	1650		
Hardness, GPa	8.3 ± 0.2	9.7 ± 0.2	10.8 ± 0.2	11.0 ± 0.2	11.4 ± 0.2		
K_{1C} , MPa.m ^{1/2}	4.4 ± 0.2	4.6 ± 0.2	5.2 ± 0.2	5.9 ± 0.2	6.2 ± 0.2		

The hardness of the ceramic is strongly correlated with its density. As the density increases, the hardness also tends to improve. This trend is consistent with the observed changes in bulk density, apparent porosity, and water absorption of the samples, indicating that higher densification contributes to enhanced mechanical properties.

4. Conclusion

In conclusion, advanced Y_2O_3 -doped SiAlON ceramics were successfully synthesized using a conventional solid-state reaction method. The effect of sintering temperature on the microstructure and properties of these ceramics was systematically investigated. This approach allows for better control over the formation of both α -SiAlON and β -SiAlON phases. Additional phases, such as $Y_2O_3 \cdot SiO_2$ and $2Y_2O_3 \cdot Al_2O_3$, were identified in specific compositions. As the sintering temperature increased from $1450\,^{\circ}$ C to $1650\,^{\circ}$ C under a nitrogen atmosphere, the bulk density of the SiAlON ceramics increased, while both porosity and water absorption decreased. The highest values of bulk density ($2.66\pm0.10\,\text{g/cm}^3$), the lowest water absorption ($2.99\pm0.20\%$), and minimal porosity ($7.95\pm0.20\%$) were observed at $1650\,^{\circ}$ C. Compared to traditional oxide powder mixing methods, this sintering approach reduced the required sintering temperature, resulting in enhanced material density (higher bulk density, lower porosity, and water absorption) and improved mechanical strength (higher hardness). The successful results of this research open up the direction of application in molten metal casting technology in the field of manufacturing automobile and motorbike parts.

Acknowledgments

The authors would like to acknowledge the Institute of Chemistry and Materials and Hanoi University of Science and Technology for their invaluable support in providing the research equipment necessary for this study.

REFERENCES

- [1] Y. K. Kshetri *et al.*, "Electronic structure, thermodynamic stability and high-temperature sensing properties of Er-α-SiAlON ceramics," *Sci. Rep.*, vol. 10, no. 1, pp. 1–13, 2020, doi: 10.1038/s41598-020-61105-z.
- [2] K. A. Kim, A. S. Lysenkov, M. G. Frolova, and Y. F. Kargin, "Effect of calcium aluminates content on the formation of Ca-α-SiAlON ceramics obtained by hot-pressing," *Ceram. Int.*, vol. 50, pp. 47886–47891,

- August 2024, doi: 10.1016/j.ceramint.2024.09.134.
- [3] A. A. M. El-Amir, A. A. El-Maddah, E. M. M. Ewais, S. M. El-Sheikh, I. M. I. Bayoumi, and Y. M. Z. Ahmed, "Sialon from synthesis to applications: an overview," *J. Asian Ceram. Soc.*, vol. 9, no. 4, pp. 1390–1418, 2021, doi: 10.1080/21870764.2021.1987613.
- [4] J. Zhou *et al.*, "The effects of in-situ SiAlON on the properties and fracture behavior of alumina-based castables: Based on microcrack toughening mechanism," *Ceram. Int.*, vol. 51, no. 4, pp. 4549–4559, 2024, doi: 10.1016/j.ceramint.2024.11.429.
- [5] M. Estili, R.-J. Xie, K. Takahashi, S. Funahashi, T. S. Suzuki, and N. Hirosaki, "Robust and orange-yellow-emitting Sr-rich polytypoid α-SiAlON (Sr₃Si₂₄Al₆N₄₀:Eu²⁺) phosphor for white LEDs," Sci. Technol. Adv. Mater., vol. 25, no. 1, 2024, doi: 10.1080/14686996.2024.2396276.
- [6] Y. Zhang *et al.*, "The synthesis of single-phase β-SiAlON porous ceramics using self-propagating high-temperature processing," *Ceram. Int.*, vol. 48, no. 3, pp. 4371–4375, 2022, doi: 10.1016/j.ceramint.2021.10.188.
- [7] T. Suehiro, N. Hirosaki, R.-J. Xie, and M. Mitomo, "Powder synthesis of Ca-α '-SiAlON as a host material for phosphors," *Chem. Mater.*, vol. 17, no. 2, pp. 308–314, 2005.
- [8] M. Z. Falak, B. A. Ahmed, H. A. Saeed, S. U. Butt, A. S. Hakeem, and U. A. Akbar, "Spark plasma sintering of SiAION ceramics synthesized via various cations charge stabilizers and their effect on thermal and mechanical characteristics," *Crystals*, vol. 11, no. 11, 2021, doi: 10.3390/cryst11111378.
- [9] M. S. Kim *et al.*, "Microstructure and mechanical properties of β-SiAlON ceramics fabricated using self-propagating high-temperature synthesized β-SiAlON powder," *J. Korean Ceram. Soc.*, vol. 54, no. 4, pp. 292–297, 2017, doi: 10.4191/kcers.2017.54.4.06.
- [10] M. Shahien, M. Radwan, S. Kirihara, Y. Miyamoto, and T. Sakurai, "Synthesis of Monolithic β-SiAlON Powders (Si_{6-z}Al_zO_zN_{8-z}, z = 2-4) through Controlling the Combustion Reaction Temperature," in *IOP Conference Series. Materials Science and Engineering (Online)*, vol. 18, 2011, doi: 10.1088/1757-899X/18/7/072003.
- [11] K. Yoshimura *et al.*, "Optical properties of solid-state laser lighting devices using SiAlON phosphor–glass composite films as wavelength converters," *Jpn. J. Appl. Phys.*, vol. 55, no. 4, 2016, Art. no. 42102.
- [12] H.-L. Li, R.-J. Xie, N. Hirosaki, T. Suehiro, and Y. Yajima, "Phase Purity and Luminescence Properties of Fine Ca-α-SiAlON:Eu Phosphors Synthesized by Gas Reduction Nitridation Method," J. Electrochem. Soc., vol. 155, no. 6, 2008, doi: 10.1149/1.2904455.
- [13] S. Zhang *et al.*, "Thermal conductivity of Ca α-SiAION ceramics with varying m and n values," *J. Am. Ceram. Soc.*, vol. 106, no. 10, pp. 5642–5647, 2023.
- [14] B. Chaudhary *et al.*, "Up- and down-conversion photoluminescence in Nd-doped SiAlON ceramics," *Ceram. Int.*, August 2025, doi: 10.1016/j.ceramint.2025.01.349.
- [15] Q. Liu, Z. Yin, F. Guo, and J. Yuan, "Effects of binary sintering additives (SmF₃-Sm₂O₃) and sintering temperature on β-SiAlON ceramic tool materials," *Ceram. Int.*, vol. 50, no. 23PB, pp. 51456–51464, 2024, doi: 10.1016/j.ceramint.2024.10.062.
- [16] X. Tian, D. Ouyang, K. Su, F. Zhao, J. Gao, and X. Liu, "Fabrication and oxidation behavior of β-SiAlON powders in presence of trace Y₂O₃," *Ceram. Int.*, vol. 48, no. 21, pp. 32464–32469, 2022, doi: 10.1016/j.ceramint.2022.07.192.
- [17] D. Bruce *et al.*, "A critical assessment of the Archimedes density method for thin-wall specimens in laser powder bed fusion: Measurement capability, process sensitivity and property correlation," *J. Manuf. Process.*, vol. 79, pp. 185–192, 2022, doi: 10.1016/j.jmapro.2022.04.059.
- [18] G. D. Quinn, "Fracture Toughness of Ceramics by the Vickers Indentation Crack Length Method: A Critical Review," *Ceramic Engineering and Science Proceedings*, vol. 27, pp. 45–62, 2008, doi: 10.1002/9780470291313.ch5.
- [19] K. Wu, L. Wu, Z. Huang, Y. Jiang, and Y. Ma, "Phase Relations in Si-Al-Y-O-C Systems," *J. Mater. Sci. Chem. Eng.*, vol. 03, no. 07, pp. 90–96, 2015, doi: 10.4236/msce.2015.37011.
- [20] Y. Zhang and A. Navrotsky, "Thermochemistry of Glasses in the Y₂O₃-Al₂O₃-SiO₂ System.," *J. Am. Ceram. Soc.*, vol. 86, no. 10, pp. 1727 1732, 2003, doi: 10.1111/j.1151-2916.2003.tb03547.x.
- [21] D. Liu, Z. Yin, F. Guo, D. Hong, and J. Yuan, "Densification, microstructure and properties of α/β-SiAlON ceramic reinforced by SiC whiskers," *Ceram. Int.*, vol. 50, no. 21PB, pp. 42755–42765, 2024, doi: 10.1016/j.ceramint.2024.08.121.
- [22] X. Li *et al.*, "Preparing β-SiAlON ceramic foam filters with high oxidation resistance," *Ceram. Int.*, vol. 49, no. 22, pp. 34510–34519, 2023, doi: 10.1016/j.ceramint.2023.08.075.
- [23] Z. Tu, X. Lao, X. Xu, W. Jiang, J. Liu, and J. Liang, "Effect of Si/Al ratio on in-situ synthesis of Al₂O₃-β-SiAlON composite ceramics for solar thermal storage by aluminothermic and silicothermic nitridation," *Ceram. Int.*, vol. 49, no. 14, pp. 22970–22978, 2023, doi: 10.1016/j.ceramint.2023.04.122.